

*Letter to the Editor***BeppoSAX observation of 3C273: broadband spectrum and detection of a low-energy absorption feature**

P. Grandi¹, M. Guainazzi^{2,1}, T. Mineo³, A.N. Parmar⁴, F. Fiore^{2,5}, A. Matteuzzi², F. Nicastro¹, G.C. Perola⁶, L. Piro¹, M. Cappi^{7,8}, G. Cusumano³, F. Frontera⁹, S. Giarrusso³, E. Palazzi⁵, and S. Piraino³

¹ Istituto di Astrofisica Spaziale, C.N.R., Via Enrico Fermi, 21 I-00044 Frascati (RM), Italy

² BeppoSAX Science Data Center, c/o Nuova Telespazio, Via Corcolle 19 I-00131 Roma, Italy

³ Istituto di Fisica Cosmica ed Applicazioni dell'Informatica C.N.R., Via Ugo La Malfa 153, I-90146, Palermo, Italy

⁴ Astrophysics Division, Space Science Department of ESA, ESTEC, Postbus 299, 2200 AG Noordwijk, The Netherlands

⁵ Osservatorio Astronomico di Roma, Via dell'Osservatorio, I-00044, Monteporzio Catone, Italy

⁶ Dipartimento di Fisica "E. Amaldi", Università degli Studi "Roma 3", Via della Vasca Navale 84, I-00146, Roma, Italy

⁷ Istituto di Tecnologie e Studio delle radiazioni Extraterrestri C.N.R., Via P.Gobetti 101, I-40129, Bologna, Italy

⁸ The Institute of Physical and Chemical Research (RIKEN), Wako-shi, Saitama, 350-01, Japan

⁹ Dipartimento di Fisica, Università di Ferrara, Via Paradiso 11, I-44100 Ferrara, Italy

Received 3 June 1997 / Accepted 26 June 1997

Abstract. We report the results of a 3C273 observation performed during the Science Verification Phase (SVP) of the *BeppoSAX* satellite. The broad-band spectrum is well represented by a power-law between ~ 1 keV and 200 keV. The spectral slope is flat ($\Gamma \sim 1.6$), with a weak emission line at ~ 6.4 keV (rest frame) of EW ~ 30 eV. Below 1 keV, a deviation from a power-law due to an absorption feature plus a soft component is present. This is the first time that a feature in absorption at ~ 0.5 keV (observer frame) is unambiguously detected in 3C273.

Key words: X-ray: observations – Quasar: 3C273

1. Introduction

3C273 is a bright, relatively nearby ($z = 0.158$) quasar and therefore has been very well studied at all wavelengths from radio to γ -rays. It is a core-jet radio source characterized by a compact nucleus and a jet showing superluminal motion. Multi-frequency campaigns have recently shown that at least 3 maxima characterize the Spectral Energy Distribution (SED) of this object, the emission peaking in the IR, in the UV and in the γ -rays (Lichti et al. 1995, von Montigny et al. 1997). The complexity of the spectrum indicates that several physical mechanisms contribute to the continuum. It is generally believed that synchrotron emission dominates the spectrum from radio to IR frequencies

(Robson et al. 1993), thermal emission is responsible for the UV bump (Ulrich et al. 1988) and inverse Compton emission produces the observed spectrum from a few keV up to GeV energies (von Montigny et al. 1997 and references therein). In the 2–10 keV region, 3C273 is represented by a power-law which extends up to ~ 1 MeV, where a break has been recently detected by OSSE (McNaron-Brown et al. 1995). The presence of a reflection component, similar to that observed in Seyfert galaxies, was suggested by GINGA data (Williams et al. 1992), but has never been confirmed. On the contrary, the iron line at 6.4 keV (rest frame) detected by GINGA, when the source was at a very low flux level, was later confirmed by ASCA (Cappi & Matsuoka 1996). At low energies, EXOSAT and ROSAT found evidence of a strong excess, usually parameterized by power-law or thermal models (Turner et al. 1990; Leach et al. 1995; Laor et al. 1994). Here we will show that the low-energy spectrum of 3C273 is actually more complex than implied by previous observations. Below 1 keV, the *BeppoSAX* data show a clear feature in absorption and a soft component. This is the first time that an absorption feature at ~ 0.5 keV (observer frame) is unambiguously detected in the 3C273 spectrum.

2. Observations and Data Reduction

3C273 was observed during the Science Verification Phase (SVP) from 1996 July 18 to July 21 with the NFI of the *BeppoSAX* satellite. The NFI consist of four co-aligned detectors: the Low Energy Concentrator Spectrometer (LECS: 0.1–10 keV; Parmar et al. 1997), the Medium Energy Concentrator Spec-

trometer (MECS: 1–10 keV) (Boella et al. 1997), the High Pressure Gas Scintillation Proportional Counter (HPGSPC: 4–120 keV; Manzo et al. 1997) and the Phoswich Detector System (PDS: 15–300 keV; Frontera et al. 1997).

All instruments operated in default configuration and data were telemetred in direct modes. Standard data selection criteria were applied¹. LECS, MECS and PDS data were reduced using SAXDAS v.1.1.0 package. For HPGSPC data, XAS v.2.0.1 package (Chiappetti 1996) was used. Data analysis was performed using the XANADU package. Total usable exposure time was 12 ksec, 131 ksec, 32 ksec and 64 ksec for LECS, MECS, HPGSPC and PDS, respectively. The short LECS exposure is due to the LECS being operated only during spacecraft night. In the LECS image the source was about 2' away from the center of the field of view and was partially obscured by a coarse strongback structure.

The LECS and the three MECS spectra were accumulated on circular regions of 8' and 4' radius, respectively. Background spectra were extracted from blank fields observations in the same position of the source. HPGSPC and PDS net source spectra and light curves were produced by subtracting the off- from the on-source products. A discussion of the systematics associated with such a procedure can be found in Manzo et al. (1997) and Matt et al. (1997) respectively.

The spectra of all the instruments were rebinned to achieve at least 20 counts per bin, in order to ensure the applicability of χ^2 test in the spectral fits. Publicly available matrices (1996, December 31 release) were used for all the instruments but the LECS, for which an *ad hoc* effective area was used to account for the offset of the source centroid.

3. Results

A monotonic trend was observed in the MECS light curve (1.5–10 keV) with the intensity decreasing by $\sim 15\%$ during the pointing. No associated spectral variability was detected.

3.1. The continuum shape above 0.8 keV

We fitted a simple power-law model, absorbed by a neutral column density N_H , separately to the spectra of the four detectors. The results are summarized in Table 1. The column density was constrained to the Galactic value ($N_H^{Gal} = 1.68 \times 10^{20} \text{ cm}^{-2}$, Savage et al. 1993). Hereafter statistical uncertainties are 90% confidence level for one interesting parameter ($\Delta\chi^2 = 2.706$).

This simple parameterization is a fairly good representation of the spectral shape in the MECS, HPGSPC and PDS. Spectral indices are consistent with each other within the statistical uncertainties. In the LECS data, instead, a deviation from the simple power-law behaviour is present below $E \sim 0.8$ keV, and is responsible for a rather high χ^2 ; spectral behaviour in this band will be discussed in §3.2. The LECS spectral slope is flatter than the MECS one in the overlapping energy band

¹ see <http://www.sdc.asi.it/software/cookbook> as a reference about data analysis software, reduction/analysis procedures and calibrations

Table 1. Power-law fits to single detectors spectra. Γ is the photon spectral index. Column density has been held fixed to the Galactic value $N_H^{Gal} = 1.68 \times 10^{20} \text{ cm}^{-2}$. N/N_{MECS} is the relative normalization at @ 1 keV from the simultaneous fit of all the instruments.

Detector	Γ	$\chi^2/\text{d.o.f}$	N/N_{MECS}
LECS (0.12–9.5 keV)	1.48 ± 0.03	329/265	...
LECS (0.8–4 keV)	$1.52^{+0.07}_{-0.08}$	153/141	0.76 ± 0.04
MECS (1.5–10 keV)	1.57 ± 0.01	191/181	1.0
HPGSPC (7–60 keV)	1.5 ± 0.3	239/211	1.07 ± 0.09
PDS (20–200 keV)	$1.60^{+0.09}_{-0.07}$	84/122	0.73 ± 0.04

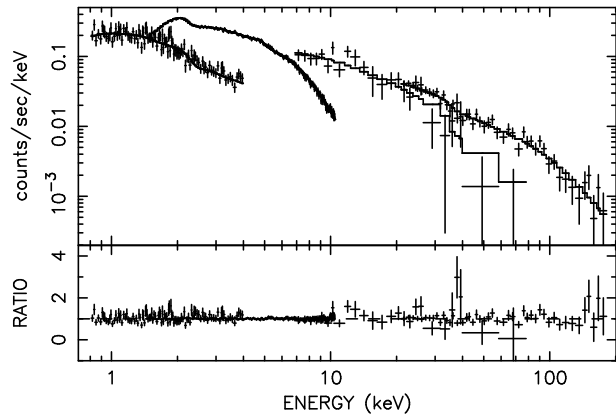


Fig. 1. Broadband 3C273 spectrum (*upper panel*) and the residuals (*lower panel*) when a simple absorbed ($N_H = N_H^{Gal}$) power-law model is applied in the 0.8–200 keV energy range.

($\Gamma_{2-9.5 \text{ keV}}^{LECS} = 1.34 \pm 0.07$). This effect has been revealed in several sources observed by *BeppoSAX* so far and is probably due to a combination of penetration in the driftless LECS gas cell (see Parmar et al. 1997) and obscuration by a window support structure rib. If the LECS data are fitted in the 0.8–4 keV energy range, the spectral index is consistent with the MECS slope, within the statistical uncertainties (see Table 1).

We then fitted the power-law model simultaneously to the data of the four detectors (0.8–200 keV), restricting the LECS data to the 0.8–4 keV band. The resulting normalization factors are different in the four instruments: their values with respect to the MECS (N/N_{MECS} in Table 1) are consistent with those obtained in the calibration performed on the Crab nebula (Cusumano et al. 1997). The fit is acceptable, $\chi^2/\text{d.o.f} = 628/621$, (see Figure 1), the spectral photon index is $\Gamma = 1.57 \pm 0.01$ and the unabsorbed flux in 2–10 keV is $F = (7.1 \pm 0.2) \times 10^{-11} \text{ erg cm}^{-2} \text{ s}^{-1}$.

3.2. Spectral features below 0.8 keV

As mentioned in the previous section, strong deviations from a simple power law model are present in the 3C273 spectrum below 0.8 keV. When a power law is fitted to the LECS data (0.12–4.0 keV), fixing the photon index to the average broadband slope ($\Gamma = 1.57$) and the cold absorber to the Galactic value, the χ^2 is unacceptable ($\chi^2/\text{d.o.f} = 259/196$). The inspection of

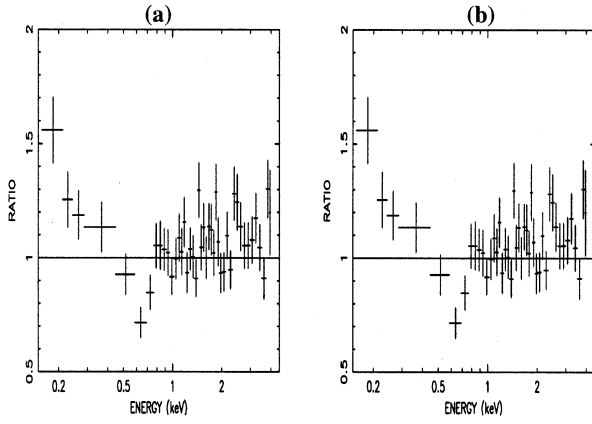


Fig. 2. An absorption feature and a soft excess are clearly evident in the LECS residuals when a power law ($\Gamma = 1.57$, $N_H = N_H^{Gal}$) is fitted the the data (*left panel*). Data are well parameterized by a broken power-law plus a notch (*right panel*)

Table 2. Best fit parameters of the soft emission when a broken power-law model + a feature in absorption are applied to the LECS data in the 0.1–4 keV band. E_{break} was fixed to the best-fit value 0.30 keV to calculate the statistical uncertainties. $N_H = N_H^{Gal}$, $\Gamma_{hard} = 1.57$ (fixed).

	Γ_{soft}	E^a (keV)	$\tau/Width$ (eV)	$\chi^2/d.o.f$
BPL	$3.0^{+0.4}_{-0.5}$	238/194
BPL + Edge	$2.7^{+0.4}_{-0.5}$	$0.61^{+0.09}_{-0.05}$	0.7 ± 0.3	210/192
BPL + Notch	$2.8^{+0.4}_{-0.5}$	$0.81^{+0.04}_{-0.06}$	64 ± 22	210/192

^a - Rest frame energy

the residuals clearly shows a photon deficit around $E \sim 0.6$ keV and an excess emission below ~ 0.3 keV (Fig.2, left panel).

We first parameterized the continuum with a broken power-law ($\Gamma_{hard} = 1.57$) and then added an absorption feature using an absorption edge or a rectangular trough profile (model NOTCH in XSPEC). We fixed the notch covering fraction equal to 1 since it was not possible to simultaneously determine meaningful constraints on its depth and width. The broken power law alone can not adequately reproduce the LECS data (see Table 2). Adding either an edge or a notch yields a statistically significant improvement $\chi^2 = 28$ (Fig.2, right panel) in both cases. Equally acceptable fits are obtained when a power law ($\Gamma_{soft} \simeq 5.0 - 5.5$) or a blackbody ($T \simeq 20$ eV) are used to describe the soft excess. Similar absorption best-fit parameters are obtained. In Table 2 the best-fit parameters are quoted for the broken power-law case (hereafter energies are quoted in the source rest frame).

3.3. Iron Line Emission

In the MECS spectrum there is evidence of an emission line around $E \sim 5.4$ keV. If a Gaussian profile is added to the power-law model in the MECS spectrum, the χ^2 is reduced by $\Delta\chi^2 = 15$, with best-fit (rest frame) parameters: $E = 6.22 \pm 0.12$

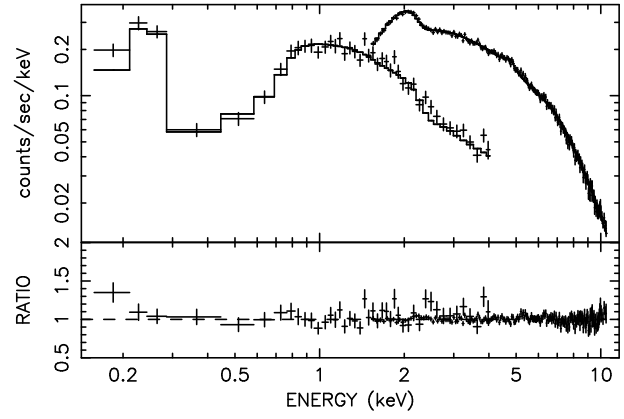


Fig. 3. Spectrum (*upper panel*) and residuals (*lower panel*) when a double power-law model is applied to the spectrum of 3C273 in the 0.12–10 keV band.

keV and $EW = 30 \pm 12$ eV. In order to test the influence of minor miscalibration around the nearby Xenon edge ($E_{Xe} \simeq 4.7$ keV), we have divided the MECS 3C273 spectrum by the Crab spectrum and inspected the residuals around the line energy. The line structure is still present and a Gaussian fit yields an $EW = 26 \pm 13$ eV. The line can be naturally explained as K_α fluorescence from neutral or mildly ionized iron, in agreement with the outcome by GINGA (Williams et al. 1992) and ASCA (Cappi & Matsuoka 1996).

4. Discussion

We have presented the results of the *BeppoSAX* observation of 3C273 during the SVP. The overall continuum is well represented by a simple power-law from ~ 1 keV to 200 keV. A weak iron line is observed in the MECS spectrum. Below 1 keV, The LECS data show a soft excess and a feature in absorption.

A non-thermal origin for the hard X-ray/ γ -photons has been suggested so far. Arguments based on the observed γ -rays luminosity and rapid X-ray variability show that the radiation must be relativistically beamed (Lichti et al. 1995). Relativistic electrons associated with the jet upscatter lower energies photons located in the same jet (synchrotron radiation, Maraschi et al. 1992; Bloom & Marscher 1993) or/and coming from the accretion disk (Dermer et al. 1992) or from the Broad Line Region (Sikora et al. 1994). If this picture is a realistic representation of 3C273, the weak line ($EW \sim 30$ eV) can be interpreted as a typical K_α iron line from accretion disk, diluted by a strong Doppler-enhanced continuum. An underlying 'Seyfert like' component is then expected to take part to the X-ray emission. The amount of such a contribution can be deduced by comparing the EW of the observed line with the typical EW (~ 200 eV) of the same line in Seyfert 1 galaxies (Nandra and Pounds 1994). It turns out to be $\sim 15\%$ at 6 keV.

We explored whether the Seyfert-like component can at least partially account for the observed soft excess. The LECS+MECS spectra were modeled with a double power-law plus a notch with fixed Galactic absorber. One power law

slope was left to vary, the other one was fixed to the typical Seyfert 1 photon index ($\Gamma_{unbeamed} = 2$). The fit result is: $\Gamma_{beamed} = 1.52_{-0.04}^{+0.05}$, $N_{unbeamed}/N_{beamed} = 10 \pm 6\%$ @ 6.4 keV ($\chi^2=411/381$ d.o.f.). The notch parameters are consistent with the ones in Table 2. We conclude that an unbeamed underlying component could account for the observed soft excess, although a residual contribution from the hard tail of the UV bump cannot be completely ruled out (Fig. 3).

We also report the detection of an absorption feature in the soft X-ray spectrum of 3C273. Such a feature can be modelled either with an absorption edge or with a notch. No discrimination between the two models can be made on statistical basis.

In the former case, the best-fit energy is consistent with the OIII-OV ionization stages at the source rest frame. We used Cloudy (version 90.01) to simulate absorption from gas characterized by a low ionization state, in order to reproduce the observed features. The ionizing continuum was described by a broken power law, as indicated by the *BeppoSAX* data, with the softer part (spectral index $\Gamma = 3$) extrapolated to lower energies to represent the UV continuum. The model can reproduce the observed feature, but, in addition, predicts strong absorption due to C (IV,V) and N (IV,VI) and HII below 0.5 keV, in completely disagreement with the excess emission present in the LECS data.

A possibility is that the absorption edge is produced by highly ionized oxygen (OVII, OVIII), as usually observed in Seyfert 1 galaxies. In this case, the gas is required to inflow ($v_{inflow}/c \sim 0.19 - 0.4$) to explain the *redshifted* position of the feature

Alternatively, the notch structure might be due to highly ionized Oxygen (the most likely candidate being the OVIII Ly- α) as suggested for PKS2155-304 (Canizares & Kruper 1984; Madjeski et al. 1991, Giommi et al. 1997). In such a case, high-velocity material ($v_{outflow}/c \sim 0.15 - 0.30$) within the jet might produce the *blueshifted* absorption through.

Acknowledgements. We would like to acknowledge all the members of the *BeppoSAX* team, whose work has allowed a successful launch and management of the mission. We would like to also thank L. Maraschi for many useful discussions.

References

- Bloom S.D. and Marscher A. P., 1993 *AIP Conf. Proc.*, 232, 34
 Boella G., Chiappetti L., Conti G., et al., 1997, *A&A* 122, 327
 Canizares C.R. and Kruper J., 1984, *ApJ* 278, L99
 Cappi M., Matsuoka M., 1996, Proceedings of the 2nd Integral Workshop “*The transparent Universe*”, S^t Malò, France
 Chiappetti L., 1996, Proceedings of the VIII Conference “*Data Analysis in Astronomy*”, Erice, Italy
 Cusumano G., Dal Fiume, Giarrusso, S., et al., 1997, *A&A* submitted
 Frontera F., Costa E., Dal Fiume F., et al., 1997, *A&A*, in press
 Giommi P., Fiore F., Grandi P., et al., in preparation
 Laor A., Fiore F., Elvis M., et al., 1994, *ApJ* 435, 611
 Leah C.M., I.M.M^cHardy, I.E. Papadakis, 1995, *MNRAS* 272, 221
 Lichti G.G., Balonek, T., Courvoisier T.J.-L et al., 1995, *A&A* 298, 711
 Madejski G.M., Mushotzky R.F., Weaver K.A., 1991, *ApJ*. 370, 198
 Manzo G., Giarrusso S., Santangelo A., et al., 1997, *A&A*, in press
 Maraschi L., Ghisellini G., Celotti A., 1992, *ApJ* 397, L5
 Matt G., Guainazzi M., Frontera F., et al., 1997, *A&A* submitted
 McNaron-Brown K., Johnson W.N., Jung G. V., et al., 1995 *ApJ* 451, 575
 Nandra K. and Pounds K.A., 1994, *MNRAS* 268 405
 Parmar A.N., Martin D.D.E., Bavdaz M., et al., 1997, *A&A*, in press
 Robson E. I., Litchfield, W.K., Gear W.K., et al., 1993 *MNRAS* 262, 249
 Savage B. D., Lu L., Bahcall J.N., et al., 1994, *ApJ* 413, 116
 Sikora M., Begelman M.C. and Rees M.J., 1994, *ApJ* 421,153
 Turner M.J.L., Williams O.R., Courvoisier T.J.L et al., 1990 *MNRAS* 244, 310
 Ulrich M.-H., Courvoisier T.J.L. Wamsteker W., 1988 *A&A* 204, 21
 Von Montigny C., Aller H., Aller M., et al. 1997 *ApJ* in press
 Williams O.R., Turner M.J.L., Stewart G.C., et al. 1992 *ApJ* 398, 157